

Accelerator-Aware Pruning for Convolutional Neural Networks

Hyeong-Ju Kang, *Member, IEEE*

Abstract—Convolutional neural networks have shown tremendous performance capabilities in computer vision tasks, but their excessive amounts of weight storage and arithmetic operations prevent them from being adopted in embedded environments. One of the solutions involves pruning, where certain unimportant weights are forced to have a value of zero. Many pruning schemes have been proposed, but these have mainly focused on the number of pruned weights, scarcely considering ASIC or FPGA accelerator architectures. When a pruned network is run on an accelerator, the lack of the architecture consideration causes some inefficiency problems, including internal buffer misalignments and load imbalances. This paper proposes a new pruning scheme that reflects accelerator architectures. In the proposed scheme, pruning is performed so that the same number of weights remain for each weight group corresponding to activations fetched simultaneously. In this way, the pruning scheme resolves the inefficiency problems, doubling the accelerator performance. Even with this constraint, the proposed pruning scheme reached a pruning ratio similar to that of previous unconstrained pruning schemes, not only on AlexNet and VGG16 but also on state-of-the-art very deep networks such as ResNet. Furthermore, the proposed scheme demonstrated a comparable pruning ratio on compact networks such as MobileNet and on slimmed networks that were already pruned in a channel-wise manner. In addition to improving the efficiency of previous sparse accelerators, it will be also shown that the proposed pruning scheme can be used to reduce the logic complexity of sparse accelerators. The pruned models are publicly available at <https://github.com/HyeongjuKang/accelerator-aware-pruning>

Index Terms—Deep learning, convolutional neural networks, neural network pruning, neural network accelerator

I. INTRODUCTION

CONVOLUTIONAL neural networks (CNNs) are attracting interest in the fields of image recognition [1]–[5], object detection [6]–[10], and image segmentation [11]. Although they provide great performance for computer vision tasks, there are certain obstacles that must be overcome before they can be adopted in embedded environments. A CNN usually requires excessive amounts of weight storage and arithmetic operations. For fast processing and low power consumption under these requirements, ASIC or FPGA accelerators have been proposed [12]–[18], but the amounts of weights and operations remain a major concern.

Manuscript received XXXXX, XX, XXXX; revised XXXXX XX, XXXX. This work was supported by Basic Science Research Program through the National Research Foundation of Korea (NRF) funded by the Ministry of Education(2015R1D1A1A01058768). This work was also supported by IDEC (EDA Tool).

H.-J. Kang is with the School of Computer Science and Engineering, Korea University of Technology and Education, Cheonan, Chungnam, 31253 Republic of Korea e-mail: hjkang@koreatech.ac.kr.

The weight amounts can be reduced by network pruning [19]–[33], where some unimportant weights are forced to have a value of zero. Multiplication with zero is meaningless, implying that reductions in operation amounts can be expected as well. Various pruning schemes have been proposed, some of which prune the weights without constraints [19], [20] while others prune the weights considering the neural network structures. It is known that relatively more weights can be pruned in fully-connected layers than in convolutional layers. However, pruning convolutional layers can reduce more energy and realize higher throughput [21]. Given that the operational structure of convolutional layers is more complex than that of fully-connected layers, convolutional layers have a greater variety of pruning schemes [22]–[32].

Pruned networks can be executed on certain ASIC or FPGA accelerators that can exploit the weight sparsity. The EIE proposed in [34] used the sparsity of weights generated by the pruning algorithm of [20], but the architecture only processes fully-connected layers. The EIE architecture was modified for a long short-term memory (LSTM) network to become the ESE architecture [35]. Cambricon-X is an architecture that can exploit weight sparsity in convolutional layers [36]. SCNN proposed in [37] exploits both weight sparsity and activation sparsity for convolutional layers. In ZENA proposed in [38], good operating efficiency was reached by skipping zero weights and activations.

Despite the various pruning schemes and accelerators, it remains challenging to utilize the performance of ASIC or FPGA accelerators efficiently with pruned networks. The aforementioned pruning schemes were developed without considering the concept of accelerator acceptability. They mainly focused on the amount of weight that can be pruned away. Pruning with no constraints creates irregular patterns in the remaining non-zero weights. These irregular patterns cause some degree of inefficiency when the pruned networks are performed on accelerators. The misalignment of the fetched activations and weights requires padding-zero insertions. The processing elements (PEs) process different numbers of weights, meaning that some PEs must wait for other PEs to complete, known as the load-imbalance problem. To alleviate these problems, some accelerators use complex structures. For example, Cambricon-X uses very wide (256×16 -bits width) memory and very wide (256-to-1) multiplexers (MUXs).

This paper proposes a new approach, a pruning algorithm which considers the accelerator architecture. There can be various architecture consideration points, and this paper will focus on the activation groups fetched and processed simultaneously in a PE and the number of remaining weights for each

group. These points are related to certain critical parameters in accelerator designs, including the number of multipliers and the width of the internal weight buffer. In the proposed algorithm, pruning is applied to weight groups, each of which corresponds to an activation group fetched together, and after pruning, a fixed number of weights remain in a group. Because pruning is applied to a weight group aligned with the operating boundary of a PE, the scheme can resolve the misalignment problem, removing waste of the internal buffer or multipliers. The pruning group can be adjusted to reduce the complexity of the data selection and indexing logic. Furthermore, since the remaining non-zero weights are distributed evenly, the load-imbalance problem can be solved naturally.

This paper is organized as follows. Section II explains CNNs, the previous pruning schemes, and the accelerator architectures. The accelerator-aware pruning scheme is proposed in Section III, and the experimental results are shown in Section IV. Section V makes the concluding remarks.

II. CNN AND PRUNING

A. CNN

A CNN usually consists of many convolutional layers and a few fully-connected layers. Between the layers, there are activation layers such as rectified linear units (ReLUs), pooling layers, and batch-normalization layers. It is known that the convolutional layers account for more than 90% of the arithmetic operations. Because the fully-connected layers require much more weight storage, recent CNNs have tended to have only one fully-connected layer [3], [4] or none [5].

The operation in a convolutional layer is as follows:

$$fo(m, y, x) = \sum_{c=0}^{C-1} \sum_{i=0}^{K-1} \sum_{j=0}^{K-1} weight(m, c, i, j) \times \quad (1)$$

$$fi(c, S \times y + i, S \times x + j) + bias(m),$$

where $fo(m, y, x)$ is the activation of row y and column x in output feature map m , and $fi(c, h, w)$ is the activation of row h and column w in input feature map c . In the equation, C is the number of the input feature maps or channels, K is the spatial size of the kernel, and S is the stride size. The $weight(m, c, i, j)$ variables are the convolution weights, and the $bias(m)$ variables are the bias terms. Fig. 1 shows the structure of the weights, consisting of M filters with a spatial size of $K \times K$ and a depth of C .

For ease of discussion, some axes are defined. The channel axis of the input activations denotes the $fi(c, h, w)$ variables with identical values of h and w . Similarly, the channel axis of the weights is defined by the $weight(m, c, i, j)$ entries with the same m, i , and j values. The spatial axis represents $fi(c, h, w)$ variables with the same c values or $weight(m, c, i, j)$ variables with identical values of m and c as well. The filter axis denotes $weight(m, c, i, j)$ variables with the same c, i , and j values. Fig. 1 shows the weights along each axis.

B. Pruning

The pruning of neural networks removes some of the unimportant weights or nodes to reduce the amount of storage

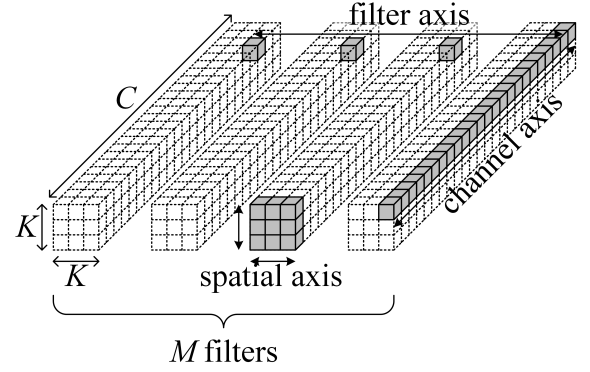


Fig. 1. Weight structure of a convolutional layer.

TABLE I
PRUNING RATIO OF THE PREVIOUS PRUNING SCHEME IN [19]

| | Conv1 | Conv | FC1&FC2 | FC3 |
|---------|-------|--------|---------|-----|
| AlexNet | 16% | 62–65% | 91% | 75% |
| VGG16 | 42% | 47–78% | 96% | 77% |

TABLE II
PREVIOUS STRUCTURED PRUNING SCHEMES

| Granularity | Pruned weights | References |
|-----------------------------|--|------------|
| channel-wise or filter-wise | $weight(:, n, :, :)$ or $weight(m, :, :, :)$ | [22]–[27] |
| shape-wise or GPU-aware | $weight(:, n, i, j)$ | [28], [29] |
| 2D/1D granularity | $weight(m, n, :, :)$ $weight(m, n, i, :)$ $weight(m, n, :, j)$ | [30] |
| SIMD aware | | [25] |

and the number of operations. The early works were presented in [39]–[41], and pruning in CNNs was proposed in [19], whose pruning results are summarized in Table I. The table shows the ratio of the pruned weights at the first convolutional layer, the other convolutional layers, the first and second fully-connected layers, and the last fully-connected layer of AlexNet and VGG16. This work was expanded with quantization and Huffman coding in [20] and with an accelerator architecture for pruned fully-connected layers in [34]. The pruning scheme can prune many weights but shows irregularities in the pruned pattern. Moreover, the corresponding accelerator architecture can only deal with fully-connected layers. The energy-aware pruning scheme proposed in [21] focuses on convolutional layers because convolutional layers consume more energy. However, this work did not consider the regularity of the pruning pattern, either.

The regularity of the pruning was considered in [22]–[31]. The pruning schemes in these studies can be categorized as channel-wise, filter-wise, and shape-wise pruning, as shown in Table II. In channel-wise pruning, for example, all of the weights in a channel are pruned or not together. These pruning schemes are referred to as structured pruning schemes, whereas pruning schemes with no constraint, as presented in [19], [20], are termed unstructured pruning.

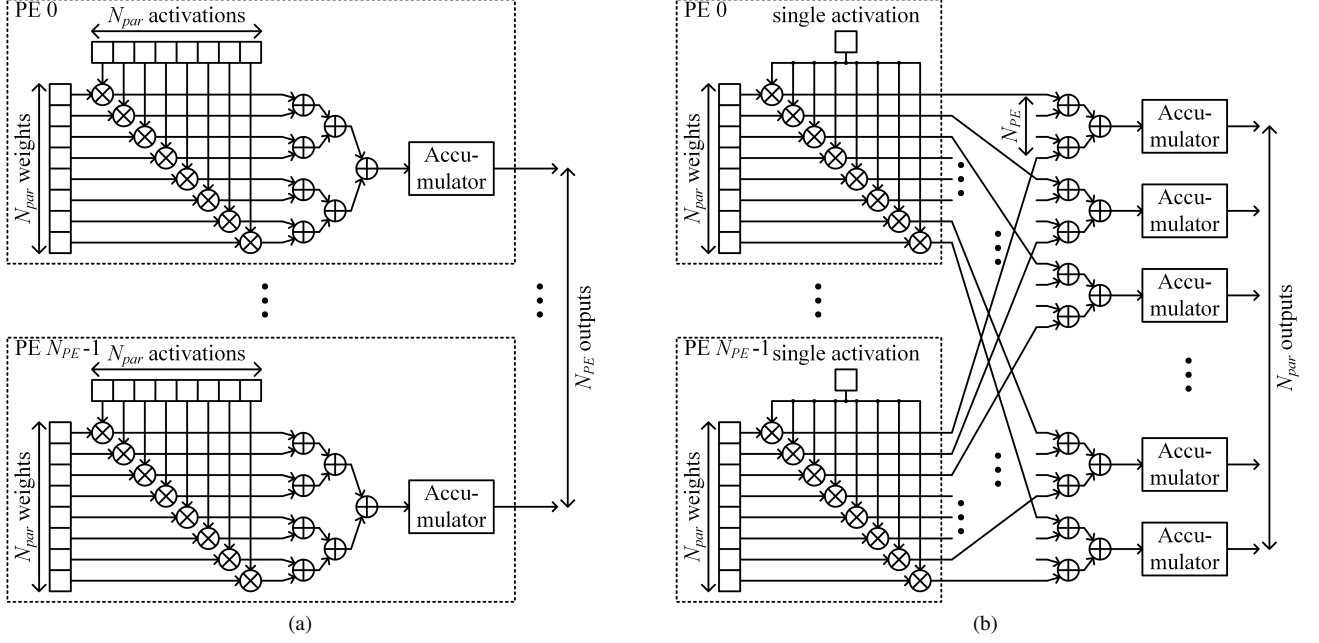


Fig. 2. Typical PE structures: (a) MWMA and (b) MWSA.

C. Neural Network Accelerators

Some ASIC or FPGA accelerator architectures have been proposed for unpruned, dense CNNs, which will be called dense architectures. An accelerator usually consists of several processing elements (PEs), each of which has a single multiplier or many multipliers. In a PE with many multipliers, the multipliers may multiply multiple weights and multiple activations (MWMA), multiple weights and a single activation (MWSA), or a single weight and multiple activations (SWMA). The MWMA and MWSA structures are shown in Fig. 2, where N_{PE} PEs operate in parallel. With the same naming convention, a PE with a single multiplier can be called a single weight and single activation (SWSA) structure.

If a PE has multiple multipliers, it is important to fetch the operands of the multipliers simultaneously. In this paper, a fetching group is defined as activations or weights that are fetched and processed simultaneously in a PE. If the size of a fetching group is N_{par} and the number of multipliers in a PE is N_{mul} , N_{par} is usually equal to N_{mul} . The weights and activations are usually fetched from the internal buffers, but the buffers are not drawn in the figures.

The PE structures can be further categorized by the axis followed by the weight- and activation-fetching groups. For example, DianNao[12] adopts the MWMA structure, where some of the input activations along the channel axis are fetched and multiplied with the corresponding kernel weights. The multiplication results are summed and accumulated to be an output activation. The MWSA structure is adopted in Cnvlutin [13] to exploit the sparsity of the input activations. Multiple weights are fetched along the filter axis. The outputs of the multiplications in PEs are gathered into $N_{par} \times N_{PE}$ -input adder trees. The architectures proposed in [16], [17] consist of MWMA-structured PEs and fetch the activations and weights

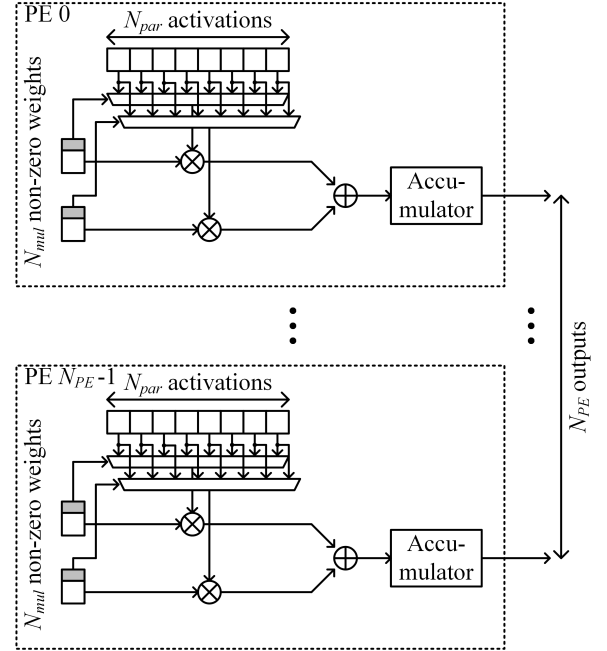


Fig. 3. Sparse MWMA PE structure.

along the spatial axis.

D. Sparse Accelerator Architectures

The architectures in Fig. 2 can be modified to exploit the weight sparsity, which will be called sparse architectures. In such architectures, only non-zero weights are stored in the weight memories to reduce weight storage use. An example of the sparse MWMA structure is shown in Fig. 3, where N_{par} activations are fetched simultaneously. N_{par} is usually larger

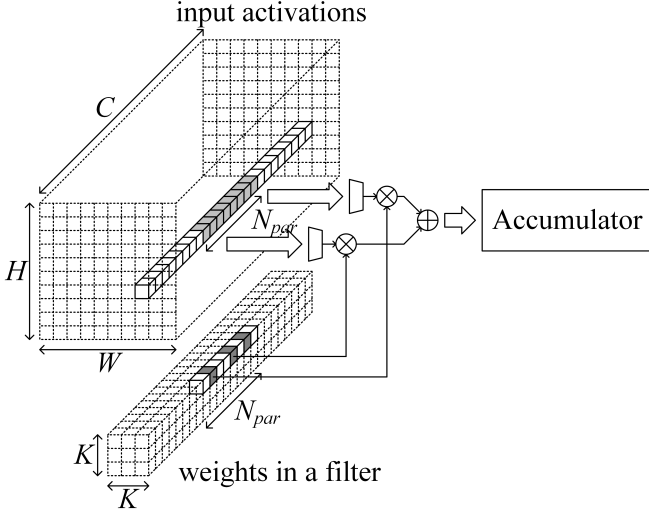


Fig. 4. Process of a sparse channel-axis-parallel CNN accelerator.

than the number of multipliers, N_{mul} , as some weights are zero and multiplications with zero weights are meaningless. Multipliers receive non-zero weights and their corresponding activations. Selecting the N_{mul} activations from the N_{par} fetched activations requires $N_{mul} \cdot b$ N_{par} -to-1 MUXs, where b is the bit width of the activations. To select a proper activation, a non-zero weight is stored with an index, denoted by the grey rectangle in Fig. 3. A process example of the sparse MWMA PE structure is illustrated in Fig. 4, where non-zero weights are shown in grey. In the figure, the upper MUX selects the second activation from the front, and the lower MUX selects the fifth activation.

As an example of such sparse architectures, Cambricon-X consists of the sparse MWMA structure PEs with $N_{par}=256$ and $N_{mul}=16$. In this architecture, 256 activations are fetched simultaneously, from which 16 activations are selected. For the selection, there are $16 \cdot b$ 256-to-1 MUXs for each PE, and the MUXs are gathered into the indexing module (IM).

For ease of discussion, the weight-fetching group in a sparse architecture is defined to include all of the zero and non-zero weights corresponding to an activation-fetching group. If the number of non-zero weights in a weight-fetching group is $N_{non-zero}$, it takes $\lceil N_{non-zero}/N_{mul} \rceil$ cycles for a PE to process the activation- and weight-fetching group. In Fig. 4, one more cycle is required to process the third non-zero weight.

Other PE structures have been used in sparse accelerators as well. EIE [34], ESE [35], and ZENA [38] adopt SWSA structured PEs to easily skip the pruned weights in the irregular pattern. SCNN [37] has multiple multipliers in a PE but exploits a special structure of Cartesian Products. In this structure, all of the fetched non-zero activations are multiplied with all of the fetched non-zero weights. The multiplication results are delivered to proper output accumulators.

E. Previous Pruning Scheme and Accelerator Architecture

Previous unstructured pruning schemes could reach high pruning ratios, but they rarely resulted in pruned networks that fit sparse accelerator architectures well. The main reason for this is the non-uniform distribution of the non-zero weights left after pruning, especially the number of non-zero weights, $N_{non-zero}$, in each weight-fetching group.

This non-uniform distribution can cause a misalignment between the activations and weights. In an accelerator with MWMA PEs, the multiplier operands should be fetched simultaneously. When N_{par} activations and N_{mul} non-zero weights are fetched from the internal buffers, it is not guaranteed that every fetched weight can find its counterpart in the fetched activations. Another activation-fetching group may have to be fetched for the process of the weights.

To solve the misalignment problem, Cambricon-X introduces a padding-zero scheme. These padding zeros, however, not only waste the internal weight buffer but also cause another type of inefficiency. The total number of padding zeros would be smaller with a larger N_{par} . This appears one of the reasons why Cambricon-X uses a very large N_{par} compared to N_{mul} . For a usual pruning ratio of 75% in convolutional layers [19], $N_{par}=64$ may be enough for $N_{mul}=16$, but Cambricon-X uses $N_{par}=256$. Due to the large N_{par} , the activation selection part, the IM block, has very wide, 256-to-1, MUXs. Because the number of the MUXs is also large, $N_{mul} \cdot b$ MUXs per PE, these wide MUXs cause a large IM block area, occupying more than 30% of the total chip area. The large N_{par} also requires a very wide ($N_{par} \cdot b$ bit-width) internal activation buffer. This type of wide memory usually induces a larger area than that associated with a square-shaped memory.

Furthermore, the load balance between PEs is also a problem. A PE processes an activation-fetching group for $\lceil N_{non-zero}/N_{mul} \rceil$ cycles. Owing to the diversity of $N_{non-zero}$, the number of cycles will vary as well. This may cause a problem in certain types of architectures such as Cambricon-X, which shares the fetched activations between PEs. If some PEs complete the process of fetched activations early, the PEs must wait for the other PEs to finish. The load-imbalance problem is also a major concern in accelerators with a weight serial structure such as the SWMA and SWSA structures [34], [35], [38].

There are few studies on pruning with considering the divergent distributions of remaining non-zero weights. The study presented in [33] considers the distribution of non-zero weights, but deals with only the fully-connected layers. Furthermore, the target was to reduce the width of the ternary weight coding without consideration of the accelerator architectures. A load-balance-aware pruning scheme was proposed in [35], but this pruning scheme focused solely on fully-connected layers, and the accelerator architecture discussion is insufficient, too. In contrast, the proposed scheme, which will be presented in the next section, is closely related to accelerator architectures, resolving all of the mentioned inefficiency problems. Furthermore, our scheme focuses on both convolutional layers and fully-connected layers.

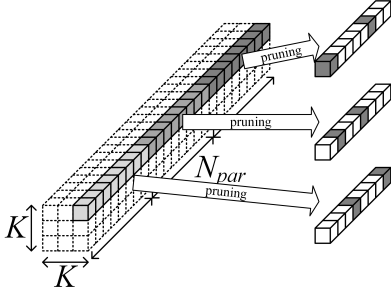


Fig. 5. Example result of the proposed pruning scheme where $N_{non-zero}=2$ for every weight-fetching group along the channel axis ($N_{par}=8$).

III. ACCELERATOR-AWARE PRUNING

In this section, we propose an accelerator-aware pruning algorithm that generates a more regular non-zero weight pattern that fits accelerator architectures well. There can be various architecture consideration points, and this paper will concentrate on two parameters, the activation- and weight-fetching groups and the number of non-zero weights left in each weight group. These two parameters are closely related to accelerator architectures. The size of the activation- and weight-fetching group determines the internal buffer width, and the number of non-zero weights is associated with the required number of multipliers and processing cycles. Previous pruning schemes do not consider these points, creating irregular distributions of the non-zero weights and the problems mentioned in the previous section. We will discuss pruning approaches for the architectures mentioned in the previous section, but the algorithm is not limited to these architectures.

A. Proposed Accelerator-Aware Pruning Scheme

In the proposed pruning scheme, the weights are pruned within the weight-fetching groups so that the number of remaining non-zero weights, $N_{non-zero}$, is uniform for all of the weight-fetching groups. The accelerator in Fig. 4, for example, simultaneously fetches and processes an activation-fetching group consisting of eight activations along the channel axis ($N_{par}=8$). $N_{non-zero}$ for the corresponding weight-fetching group is three in the figure. However, previous pruning schemes provide no guarantee for $N_{non-zero}$. $N_{non-zero}$ can be two or four in another weight-fetching group. Even zero or the size of a weight-fetching group is possible. In contrast, the proposed scheme leaves a fixed number of non-zero weights for all of the weight-fetching groups, as shown in Fig. 5. In the figure, every weight-fetching group has six weights pruned away with two non-zero weights remaining ($N_{non-zero}=2$), as indicated in white and grey, respectively.

The result of the proposed pruning scheme can be applied to the previous sparse accelerators, resolving the inefficiency problems mentioned in the previous section. The misalignment problem in the sparse MWMA and MWSA structures will be solved if the number of remaining non-zero weights per group is set to be a multiple of N_{mul} . This alignment would make the padding zeros obsolete in Cambricon-X. Furthermore, the proposed scheme can solve the load-imbalance problem,

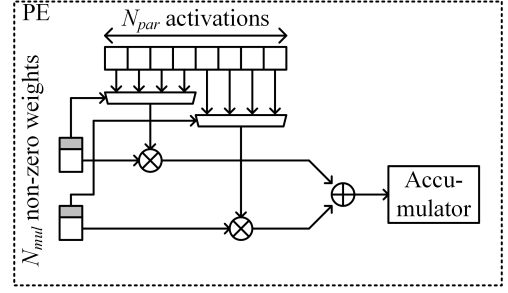


Fig. 6. PE structure when $N_{par}=8$ and $N_{group}=4$.

one of the main concerns in the weight serial structures as well. Every weight-fetching group has the same number of remaining non-zero weights, so the number of weights for a PE to process is naturally balanced if every PE processes the same number of weight-fetching groups. Every sparse architecture mentioned in the previous section can benefit from the proposed pruning scheme.

A similar scheme was presented in [33], but the regularity was used only to reduce the amount of weight storage. They did not consider the effect on the accelerator architecture. Furthermore, they only dealt with fully-connected layers. The load-balance-aware pruning scheme, proposed in [35], adopts a similar concept, but it can be thought of as a special case of the proposed scheme. The load-balance-aware pruning is also limited to fully-connected layers and the EIE and ESE architectures.

B. Accelerator Complexity Reduction

In addition to improving the efficiency of previous sparse architectures, the proposed scheme can also be used to reduce the degree of accelerator complexity, especially with regard to the indexing and activation selection logic. Cambricon-X has very wide (256-bit width) activation buffers and very wide (256-to-1) MUXs in the activation selection logic to deal with the irregular distribution of non-zero weights by the previous pruning schemes, as mentioned in Subsection II-E. The input width of the MUXs can be narrowed by the proposed pruning scheme, simplifying the activation selection logic. First, every weight-fetching group is divided evenly into g sub-groups, referred to as the pruning groups. The size of a pruning group, N_{group} , will be N_{par}/g . The pruning is then performed so that each pruning group has a constant number of weights pruned. If the number of weights pruned away in a pruning group is N_{prune} , the pruning ratio will be N_{prune}/N_{group} .

Since a weight corresponds to one of the N_{group} activations, the width of a MUX for the activation selection can be reduced to N_{group} . With the smaller N_{group} , the PE structure in Fig. 3 can be modified, becoming the structure shown in Fig. 6. As indicated in the figure, the activation selection logic becomes simplified with narrower MUXs. When N_{group} becomes smaller, however, degradation of the network performance can increase with the same pruning ratio. The experiment shows that $N_{group}=16$ with a 75% pruning ratio does not deteriorate the CNN performance.

The proposed pruning scheme can induce a reduction of N_{par} , too. As mentioned in Subsection II-E, $N_{par}=256$ for Cambricon-X is large compared to $N_{mul}=16$. $N_{par}=64$ is enough for the common pruning ratio of 75% in the convolutional layers. A large N_{par} may be chosen to reduce the number of padding zeros. However, the proposed scheme makes the padding zeros unnecessary, implying that $N_{par}=64$ can be used. In this case, the width of the activation buffers can be reduced to 64, enabling more square-like memory components to be used. Square-like memory components are more area-efficient than wide memory components.

Furthermore, the indexing logic can be simplified. For the indexing of the irregular non-zero weights, Deep Compression and EIE use relative indexing [20], [34], where the number of zero weights between two adjacent non-zero weights is stored. The interval is encoded with four bits, and an interval larger than the encoding bound requires filler zero insertion. A similar indexing scheme is used in Cambricon-X, known as step indexing. The indexing can be simplified with the proposed pruning scheme, where pruning is performed within a pruning group of N_{group} . The small N_{group} enables direct indexing, where an index indicates the position of the non-zero weight within the pruning group. Given that N_{group} is small, the indexing bit width is also small, $\lceil \log_2 N_{group} \rceil$ bits, even with direct indexing. Direct indexing is much simpler than relative indexing in EIE or step indexing in Cambricon-X and does not require filler zeros, removing the waste of the weight storage.

C. Incremental Pruning

In the proposed scheme, N_{prune} weights are pruned in a pruning group. The pruning can be processed in a few different ways. At one extreme, the target number of weights with the least magnitude are pruned at the same time in each group, and the pruned network is retrained. This scheme is called one-time pruning in this paper. At the other extreme, pruning begins with only one weight with the least magnitude in each group. Subsequently, a period of retraining is undertaken, followed by the pruning of one more weight with the least retrained magnitude. Retraining is performed again. The one weight pruning and retraining processes are iterated until the target number is reached. In the middle of the two extreme methods, we can set the initial pruning number and the increment number. This scheme is referred to here as incremental pruning.

Obviously, incremental pruning would be better than or equal to the one-time pruning method. However, incremental pruning requires a long retraining time. Accordingly, in this paper, it will be applied when one-time pruning is not sufficient.

D. Pruning for Various Architectures

In the proposed pruning scheme, pruning can be applied to CNNs for various accelerator architectures. In the previous subsections, pruning along the channel axis is shown for architectures such as Cambricon-X. As an example of pruning for another type of accelerator architecture, the proposed pruning scheme can be adjusted to a weight-sparse version

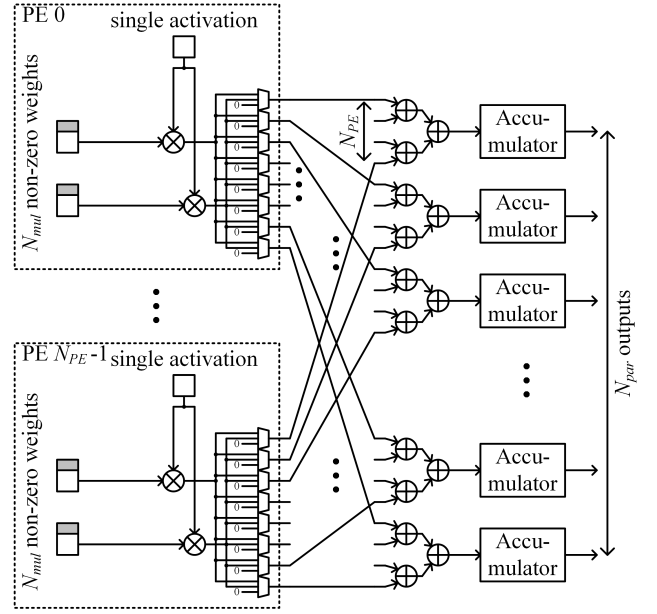


Fig. 7. Sparse MWSA PE structure.

of Cnvlutin. Cnvlutin adopts the MWSA structure, and the weights are fetched along the filter axis. In this architecture, the dense MWSA structure can be modified to the sparse MWSA structure shown in Fig. 7. For the sparse architecture, the proposed pruning scheme can be applied to CNNs with pruning groups set to the weights along the filter axis. Because Cnvlutin already exploits activation sparsity, the structure in Fig. 7 can exploit both activation sparsity and weight sparsity.

The architectures in [16], [17] adopt sparse MWMA structure PEs, where the activations and weights are fetched and processed along the spatial axis. For these architectures, the proposed pruning scheme can be applied with pruning groups established along the spatial axis.

E. Application to Fully-Connected Layers

The proposed pruning scheme can be applied to fully-connected layers as well. In a fully-connected layer, the weights can be arranged in a matrix format. We can define two axes: the column axis and the row axis. Along the row axis, the weights are multiplied with different activations, while along the column axis, the weights are multiplied with an activation. An MWMA-structured PE processes the weights along the row axis simultaneously, and an MWSA-structured PE processes the weights along the column axis.

According to the PE structures, accelerator-aware pruning is applied following different axes. If an MWMA-structured PE is used, the weights are grouped along the row axis and pruned so that each group has a fixed number of non-zero weights remaining. If an MWSA-structured PE is used, the weights are grouped and pruned along the column axis. An example of the proposed pruning scheme along the row axis is illustrated in Fig. 8. In the figure, $N_{par}=N_{group}=8$ and $N_{prune}=6$.

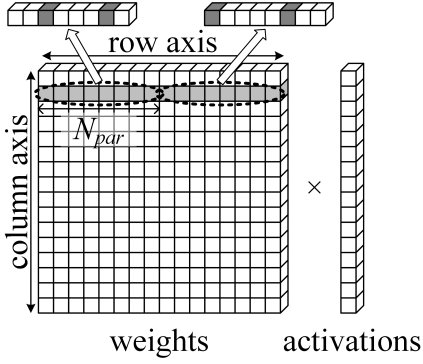


Fig. 8. Example result of the proposed pruning scheme with $N_{group}=8$ and $N_{prune}=6$ on a fully-connected layer.

IV. EXPERIMENTAL RESULTS

To show that the proposed pruning scheme can preserve the performance of CNNs well even with the given constraint, the top-5 accuracy for the ImageNet 2012 validation data set [42] was measured. The retraining was performed by Caffe [43] in one of three modes. In Retraining 1, after one-time pruning, retraining was performed with a learning rate of $5 \cdot 10^{-4}$ for 12 epochs. If the original accuracy was not recovered, 8-epoch retraining was performed additionally with a learning rate of 10^{-4} . If Retraining 1 was not enough, Retraining 2 was applied, where the learning rate begins at $5 \cdot 10^{-4}$ and decreases to 10^{-4} , 10^{-5} , and 10^{-6} when the validation accuracy becomes saturated. In Retraining 3, Retraining 2 is applied with incremental pruning. When the validation accuracy is saturated at the learning rate of 10^{-6} , N_{prune} is increased and the retraining resumes with a learning rate of $5 \cdot 10^{-4}$. The retraining mini-batch size was set to 256. The network models were obtained publicly [44]–[48]. Various methods can be used to select the weights to be pruned. Any selection method is applicable, but the simplest method was used in the experiments. The weights with the least magnitude are pruned first in a pruning group.

The pruning of convolutional layers will be discussed first because convolutional layers account for most of the computations. The proposed pruning scheme does not change the channel number of output feature maps and can therefore be applied to the residual blocks of ResNet including multiple branches without difficulty. The bias values are not pruned. Our pruning scheme was then applied to fully-connected layers with the pruned convolutional layers. It will be shown that the proposed pruning method is also applicable to compact networks. The last two subsections will analyze the effects of the proposed scheme on the accelerator performance and complexity.

A. Convolutional Layer Pruning

Table III shows the accuracy results right after the pruning of the convolutional layers. The weights are grouped along the channel axis, and the first convolutional layer is not pruned as it has a much smaller number of weights and operations than the other layers. The table shows that 30% (3/8 or 6/16)

TABLE III
IMAGE NET VALIDATION ACCURACY(%) RIGHT AFTER CONVOLUTIONAL LAYER PRUNING

| N_{group} | N_{prune}^{conv} | AlexNet | VGG16 | ResNet-50 | ResNet-152 |
|-------------|--------------------|---------|-------|-----------|------------|
| - | - | 79.81 | 88.44 | 91.14 | 92.20 |
| 8 | 1 | 79.68 | 88.31 | 90.94 | 92.12 |
| 8 | 2 | 79.17 | 88.02 | 90.30 | 91.69 |
| 8 | 3 | 76.89 | 85.52 | 88.27 | 90.72 |
| 8 | 4 | 65.02 | 70.20 | 78.79 | 86.37 |
| 8 | 5 | 32.19 | 12.23 | 17.21 | 46.58 |
| 16 | 1 | 79.83 | 88.47 | 91.16 | 92.22 |
| 16 | 2 | 79.76 | 88.36 | 91.08 | 92.18 |
| 16 | 4 | 79.35 | 88.19 | 90.80 | 92.07 |
| 16 | 6 | 78.00 | 86.64 | 88.88 | 91.36 |
| 16 | 8 | 69.99 | 75.34 | 80.74 | 87.90 |
| 16 | 9 | 60.84 | 55.15 | 59.39 | 80.36 |
| 16 | 10 | 38.61 | 20.12 | 32.42 | 65.67 |

TABLE IV
IMAGE NET VALIDATION ACCURACY(%) AFTER CONVOLUTIONAL LAYER PRUNING AND RETRAINING

| N_{group} | N_{prune}^{conv} | AlexNet | VGG16 | ResNet-50 | ResNet-152 |
|-----------------------|--------------------|---------|-------|-----------|------------|
| - | - | 79.81 | 88.44 | 91.14 | 92.20 |
| 8 | 4 | 80.45 | 90.71 | 91.95 | 93.03 |
| 8 | 5 | *80.58 | 90.45 | 91.68 | 92.79 |
| 8 | 6 | *80.42 | 89.91 | 91.14 | 92.33 |
| 8 | 7 | *79.47 | 88.48 | 88.86 | 91.00 |
| 16 | 8 | 80.46 | 90.73 | 91.96 | 93.02 |
| 16 | 9 | 80.38 | 90.80 | 91.80 | 92.89 |
| 16 | 10 | *80.62 | 90.54 | 91.86 | 92.75 |
| 16 | 11 | *80.74 | 90.38 | 91.55 | 92.55 |
| 16 | 12 | *80.50 | 90.22 | 91.35 | 92.48 |
| 16 | 13 | *80.22 | 89.65 | 90.88 | 92.20 |
| Unstructured (81.25%) | | *80.34 | 90.06 | 91.17 | 92.37 |

pruning already begins to degrade the accuracy. However, the degradation can be recovered with retraining as shown in Table IV. Retraining 1 and 3 are applied; the results of Retraining 3 are denoted by asterisks.

In the table, with up to 75% (6/8 or 12/16) pruning, the validation accuracy could be recovered to the baseline accuracy with Retraining 1 in very deep networks, including VGG16, ResNet-50, and ResNet-152. The result of VGG16 matches that of the unstructured pruning algorithm in [19], where the pruning ratios of the convolutional layers are more or less than 75% in VGG16. The experiment shows that a similar pruning ratio can be reached with the proposed pruning scheme considering the accelerator constraint. It can also be seen that a 75% pruning ratio does not degrade the accuracy in the residual networks, ResNet-50 and ResNet-152. The networks have more complicated structures, such as a residual path and 1×1 convolution. The results show that the proposed scheme can be applied to recent state-of-the-art CNNs. With some pruning ratios, the accuracy is improved, which has been observed in other pruning papers, too [19], [30]. This improvement appears to be caused by a kind of regularization [30].

In a relatively shallow network such as AlexNet, it was more difficult to recover the accuracy. With the more advanced effort of Retraining 3, however, the original accuracy level can be recovered with pruning ratios comparable to those in [19]. In AlexNet, Retraining 3 begins with $(N_{prune}, N_{group})=(5,8)$ or

TABLE V
IMAGENET VALIDATION ACCURACY(%) AFTER FULLY-CONNECTED
LAYER PRUNING AND RETRAINING WITH $N_{group}=16$ AND $N_{prune}^{conv}=12$

| $N_{prune}^{fc1,2}$ | N_{prune}^{fc3} | AlexNet | VGG16 | ResNet-50 | ResNet-152 |
|---------------------|-------------------|---------|-------|-----------|------------|
| - | - | 79.81 | 88.44 | 91.14 | 92.20 |
| 12 | 12 | *80.24 | 89.84 | 91.24 | 92.54 |
| 13 | 12 | *80.29 | 89.56 | - | - |
| 14 | 12 | *80.01 | 89.19 | - | - |
| 15 | 12 | *79.47 | 88.95 | - | - |

(10,16), and N_{prune} is increased by one. While the pruning ratio of the AlexNet convolutional layers was around 65% with the unstructured pruning in [19], the proposed scheme can reach a pruning ratio of 81.25% after approximately 300 epochs of retraining.

The last row of the table shows the results of an unstructured pruning scheme, which prune 81.25% of weights with the least magnitude in each convolutional layer. The unstructured pruning scheme shows a little better accuracies, but the differences are negligible.

B. Fully-Connected Layer Pruning

After the pruning of the convolutional layers, the fully-connected layers were pruned along the row axis. In the fully-connected layer pruning step, we attempted to prune more weights than were pruned in the convolutional layers because, generally, more weights can be pruned in fully-connected layers [19]. The size of a pruning group, N_{group} , was equally set for the convolutional layers and fully-connected layers.

The retrained accuracy is shown in Table V. In the table, N_{prune}^{conv} , $N_{prune}^{fc1,2}$, and N_{prune}^{fc3} are the number of pruned weights in the convolutional layers, the first and second fully-connected layers, and the last fully-connected layer, respectively. ResNet-50 and ResNet-152 have one fully-connected layer; hence, $N_{prune}^{fc1,2}$ was ignored in these networks. Retraining 1 was applied to all of the networks except for AlexNet, to which Retraining 3 was applied. In Retraining 3, $N_{prune}^{fc1,2}$ was increased by one from 12.

The table shows that the proposed pruning scheme can reach a pruning ratio similar to that of the previous pruning scheme in the fully-connected layers. In [19], 90–96% of the weights were pruned in the first and the second fully-connected layers of AlexNet and VGG16, and as were 75–77% of the weights in the last layer. In all of the presented networks, the proposed pruning scheme could prune 75% of the weights ($N_{prune}^{fc3}=12$) in the last fully-connected layers. For the first and second fully-connected layers of VGG16, pruning with $N_{prune}^{fc1,2}=15$ (93.75% pruning) did not degrade the accuracy. In AlexNet, $N_{prune}^{fc1,2}=15$ showed an accuracy of 79.47%, which is slightly worse than the accuracy of the pruned AlexNet in [19], 79.68%. Because $N_{prune}^{conv}=12$ in the convolutional layers is larger than 62–65% in [19], the pruning results are quite comparable.

C. Pruning Along Other Axes

The proposed pruning scheme can be applied along other axes. The accuracy results after pruning and retraining along

TABLE VI
IMAGENET VALIDATION ACCURACY(%) AFTER PRUNING AND
RETRAINING ALONG OTHER AXES

| Axis | N_{group} | N_{prune}^{conv} | VGG16 | ResNet-50 |
|---------|-------------|--------------------|-------|-----------|
| - | - | 0 | 88.44 | 91.14 |
| Filter | 16 | 10 | 90.63 | 91.71 |
| Filter | 16 | 11 | 90.46 | 91.54 |
| Filter | 16 | 12 | 90.12 | 91.31 |
| Filter# | 16 | 12 | 89.49 | 90.85 |
| Spatial | 9 | 5 | 90.32 | 91.85 |
| Spatial | 9 | 6 | 89.69 | 91.49 |
| Spatial | 9 | 7 | 88.86 | 91.31 |

TABLE VII
IMAGENET VALIDATION ACCURACY(%) AFTER PRUNING AND
RETRAINING OF COMPACT NETWORKS

| N_{group} | N_{prune}^{conv} | SqueezeNet v1.0 | MobileNetV1-224 1.0 |
|-------------|--------------------|-----------------|---------------------|
| - | - | 80.39 | 89.24 |
| 16 | 8 | *80.93 | 89.97 |
| 16 | 9 | *80.65 | 89.67 |
| 16 | 10 | *80.29 | *89.79 |
| 16 | 11 | *79.86 | *89.50 |
| 16 | 12 | *78.80 | *89.06 |

the filter and the spatial axis are presented in Table VI. At the third to fifth rows in this table, the convolutional layers are pruned along the filter axis, and at the next row, denoted by '#', the fully-connected layers are further pruned with $N_{prune}^{fc1,2}=15$ and $N_{prune}^{fc3}=12$. At the last three rows, the convolutional layers are pruned along the spatial axis. These results show that the accuracy is not degraded by pruning along other axes, meaning that the proposed accelerator-aware pruning scheme can be used for various accelerator architectures.

D. Compact Network Pruning

Some compact networks have been proposed recently [5], [49], [50]. The compact networks are less redundant, meaning that pruning may be more harmful. Table VII, however, shows that the original accuracy can be recovered with the accelerator-aware pruning along the channel axis. In SqueezeNet, the proposed scheme can reach a pruning ratio comparable to 66.3%, the pruning ratio of an unstructured pruning scheme in [5]. With $N_{prune}^{conv}=10$ or 11, the accuracy degradation of the proposed pruning scheme is around 0.5 percent points. In MobileNet [49], the accuracy is recovered more easily. In this case, 75% pruning shows still good accuracy. MobileNet consists of depthwise convolutional layers and pointwise convolutional layers, and only the latter ones were pruned because they account for most of the operations and weight storage.

E. Slimmed Network Pruning

Some previous works pruned convolutional layers in a channel-wise or filter-wise approach [22]–[24]. The resulting networks are slimmer networks with fewer channels in the layers. Slimmed networks can also be pruned by the proposed pruning scheme. For this experiment, the networks slimmed in [24] were used because their models are publicly available

TABLE VIII
IMAGE NET VALIDATION ACCURACY(%) AFTER PRUNING AND
RETRAINING OF SLIMMED NETWORKS IN [24]

| N_{group} | N_{prune}^{conv} | VGG16-4X | VGG16-5X | ResNet-50 CP |
|-------------|--------------------|----------|----------|--------------|
| - | - | 89.06 | 86.98 | 89.64 |
| 16 | 8 | 89.53 | 88.25 | 91.44 |
| 16 | 10 | 88.58 | 87.91 | 91.28 |
| 16 | 12 | *87.05 | 87.36 | 90.30 |

TABLE IX
ACCELERATOR PERFORMANCE ESTIMATION

| Architecture | | Han15[19] | Han15[19] [#] | AAP |
|------------------------|-----------------------|-----------|------------------------|-------|
| Cambricon-X Conv2-5 | $N_{nonzero}^{total}$ | 1098K | 751K | 751K |
| | $N_{padding}$ | 160K | 171K | 38K |
| | N_{MAC} | 283M | 191M | 191M |
| | N_{cycle} | 1946K | 1540K | 857K |
| | Utilization | 57% | 49% | 87% |
| EIE FC1-3 | $N_{nonzero}^{total}$ | 5925K | 4456K | 4456K |
| | N_{cycle} | 187K | 154K | 70K |
| | Utilization | 49% | 45% | 100% |

[51]. In [24], the weight amount of the networks was also reduced by other methods such as decomposition. The proposed scheme was applied with $N_{group}=16$. In some layers of the slimmed networks, C is not a multiple of N_{group} . In such a case, it is assumed that zero weights are added to make C a multiple of N_{group} .

The accuracy results are shown in Table VIII. The table presents that the proposed pruning scheme prunes weights fairly well even in the already slimmed networks. In this case, 50% pruning of the convolutional layers ($N_{prune}^{conv}=8$) does not degrade the accuracy of the slimmed networks. It was also noted that 75% pruning of $N_{prune}^{conv}=12$ does not degrade the accuracy of VGG16-5X or ResNet-50 CP.

F. Accelerator Performance

A neural network pruned by the proposed scheme can be processed more efficiently in accelerators. The upper part of Table IX compares the efficiency of Cambricon-X when it runs the second to fifth convolutional layers of AlexNet pruned by the unstructured pruning in [19] and the proposed accelerator-aware pruning. In the table, $N_{nonzero}^{total}$, $N_{padding}$, N_{MAC} , and N_{cycle} are the number of total non-zero weights after each pruning, the required number of padding zeros for the alignment, the number of multiplication and accumulation (MAC) operations with non-zero weights, and the number of estimated processing cycles, respectively. The utilization is the ratio of time when the multipliers operate with valid operands, calculated as follows:

$$\text{Utilization} = \frac{N_{MAC}}{N_{cycle} \times N_{mul} \times N_{PE}}. \quad (2)$$

With the conventional pruning scheme, Cambricon-X executes the pruned network with some inefficiency, as shown at the third column. The amount of the required padding zeros is approximately 14.6% of the non-zero weight amount, which indicates a waste of the internal buffer and the multipliers. With the additional problem of the load imbalance between PEs, the utilization of the multipliers is only 57%.

With the proposed scheme shown in the last column, the resource waste can be greatly reduced. For the column, AlexNet is pruned by the proposed scheme with $N_{prune}^{conv}=12$ and $N_{group}=16$. The amount of the padding zeros is merely 5% of the non-zero weight amount. The padding zeros are required at the second convolutional layer because this layer does not have enough input channels. With 48 input channels, only twelve non-zero weights remain for an activation-fetching group, which is less than N_{mul} . The small amount of padding zeros and the naturally load-balanced PEs lead to high utilization, at 87.24%, and the processing cycles are reduced by 56%.

Since the pruning ratio of [19] is less than 75%, we compared an additional case at the fourth column. For this column, each layer of the network at the third column is additionally pruned to reach 75% pruning ratio. With the additional pruning, the numbers of non-zero weights and MACs are reduced, but a similar number of padding zeros is still required. The utilization is deteriorated further. Compared to this case, the proposed pruning scheme can reduce the number of processing cycles by 44%.

The lower part of Table IX compares the number of processing cycles of the EIE architecture. Because the EIE architecture only deals with the fully-connected layers, the table compares the cycles processing the fully-connected layers of AlexNet. In this part, N_{MAC} and $N_{zero-pad}$ are not described because N_{MAC} is equal to $N_{nonzero}^{total}$ in fully-connected layers and EIE does not require padding zeros. In EIE, N_{PE} is 64, and each PE has a multiplier. According to the EIE process, the accelerator-aware pruning is applied along the column axis with $N_{group}=16$, $N_{prune}^{fc1,2}=15$, and $N_{prune}^{fc3}=12$. As shown in the table, the load-imbalance problem degrades the utilization to 49%. The proposed pruning scheme, shown at the fifth column, improves the utilization to 100%, reducing the number of processing cycles by around 63%. For a fair comparison, the network of the third column is pruned additionally, and the result is shown at the fourth column. With the utilization under 50%, the additionally pruned network still requires more than twice as many processing cycles as that of the fifth column.

G. Accelerator Logic Complexity

As mentioned in Subsection III-B, the proposed pruning scheme can reduce the accelerator complexity. In this subsection, attempts are made to reduce the area of Cambricon-X. The second row in Table X presents the area, delay time, and power consumption of Cambricon-X. The power values were measured with dynamic simulation. In the table, NBin, NBout, and SB are the input activation buffer, the output activation buffer, and the weight buffer, respectively. IM is the indexing and activation selection unit including the activation selection MUXs.

Because the RTL code of Cambricon-X is not publicly available, we re-implemented the blocks in the table for the area comparison. The other blocks in Cambricon-X are not affected by the proposed scheme. Hardware parameters are inferred from the context of the paper. The synthesis results of the re-implemented case are presented at the third row. The

TABLE X
ACCELERATOR SYNTHESIS RESULTS

| Accelerators (Measurement Condition) | N_{par} | N_{group} | N_{mul} | NBin | NBout | Area (mm ²) | | 16 PEs | Total | Delay (ns) | Power (W) |
|---|-----------|-------------|-----------|------|-------|-------------------------|------|--------|-------|---------------|--------------|
| Cambricon-X (P&R) | | | | 0.55 | 0.55 | 1.05 | 1.98 | 1.78 | 6.38 | 1.00 | 0.95 |
| Re-implemented (Synthesis) | 256 | 256 | 16 | 0.32 | 0.32 | 0.43 | 2.39 | 1.46 | 4.91 | 1.02 | 2.56 |
| Reduced (Synthesis) | 64 | 8 | 16 | 0.11 | 0.11 | 0.43 | 0.17 | 1.19 | 2.01 | 1.05 | 1.24 |
| Reduced (Synthesis) | 64 | 16 | 16 | 0.11 | 0.11 | 0.43 | 0.27 | 1.41 | 2.34 | 1.02 | 1.49 |
| Reduced (Synthesis) | 64 | 32 | 16 | 0.11 | 0.11 | 0.43 | 0.44 | 1.44 | 2.53 | 1.02 | 1.58 |
| Cambricon-X Reduced (Estimation) | 64 | 16 | 16 | 0.19 | 0.19 | 1.05 | 0.22 | 1.72 | 3.84 | 1.00 | 0.56 |
| Reduced (Synthesis) | 128 | 16 | 16 | 0.18 | 0.18 | 0.43 | 0.28 | 1.41 | 2.47 | 1.02 | 1.58 |
| Reduced (Synthesis) | 64 | 16 | 8 | 0.11 | 0.11 | 0.29 | 0.16 | 0.62 | 1.29 | 1.02 | 0.71 |

synthesis was performed by Synopsys DesignCompiler with the Global Foundry 65nm process library. Since the results of Cambricon-X are obtained after the placement and routing (P&R) process with a different library, it is difficult to compare the values of the second and third rows directly. Therefore, the expected reduction effect on Cambricon-X will be estimated from the reduction in the re-implemented version, which is shown at the following rows. The number of PEs, N_{PE} , is assumed to be 16.

The fourth to sixth rows present the synthesis results of reduced implementation assuming the application of the proposed pruning scheme with various N_{group} values. Compared to the results of the re-implemented Cambricon-X at the third row, the area is reduced greatly, especially that used by NBin, NBout and IM. The area of NBin and NBout is reduced due to the memory width reduction from 256×16 to 64×16 . Although the memory capacity remains unchanged, the more square-shaped memory configuration results in a smaller area. The area reduction of the IM block is more astonishing, with a decrease of 82–93%. The wide MUXs, 256-to-1 MUXs, in the IM block of Cambricon-X are substituted with narrow N_{group} -to-1 MUXs. Because the area of a MUX logic is proportional to the input width, the narrow MUXs lead to a smaller IM block. With the smaller area, the table also shows lower power consumption. The delay increased slightly, but the difference is negligible. The seventh row shows the estimated Cambricon-X when the simplification proposed in Subsection III-B is applied. The values were obtained by comparing the third and fifth rows. Due to the area reduction of NBin, NBout, and IM, the total area can be reduced by 40%.

The results of various configurations are presented at the last two rows for comparison. With $N_{par}=128$, the areas of activation memory components are increased due to wide memory configuration. The area of the IM block is not increased because the same N_{group} leads to the same MUX input width. The area of the IM block is affected by N_{group} and N_{mul} . The tables shows that N_{mul} affects the area of SB though the capacity of SB is not changed. This is also due to the memory configuration.

V. CONCLUSIONS

In this paper, an accelerator-aware pruning scheme was proposed for CNNs. In the pruning process, the proposed scheme considers the accelerator parameters: the width of the internal activation buffer and the number of multipliers. After pruning,

each weight-fetching group has a fixed number of non-zero weights left. Networks pruned by the proposed scheme can be efficiently run on the target accelerator. Furthermore, the proposed pruning scheme can be used to reduce the complexity of the accelerators, too. Even with the accelerator constraint, it was shown that the proposed scheme can reach pruning ratios close to those of existing unstructured pruning schemes. In this paper, the pruning scheme was discussed in relation to representative sparse accelerator architectures, but the scheme can be used for any sparse architectures.

REFERENCES

- [1] A. Krizhevsky, I. Sutskever, and G. E. Hinton, "ImageNet classification with deep convolutional neural networks," in *Proc. Advances in Neural Inf. Process. Syst.*, 2012, pp. 1097–1105.
- [2] K. Simonyan and A. Zisserman, "Very deep convolutional networks for large-scale image recognition," in *Proc. Int. Conf. Learning Representations*, 2015. [Online]. Available: <http://arxiv.org/abs/1409.1556>
- [3] C. Szegedy, W. Liu, Y. Jia, P. Sermanet, S. Reed, D. Anguelov, D. Erhan, V. Vanhoucke, and A. Rabinovich, "Going deeper with convolutions," in *Proc. Comput. Vision and Pattern Recognition*, 2015, pp. 1–9. [Online]. Available: <http://arxiv.org/abs/1409.4842>
- [4] K. He, X. Zhang, S. Ren, and J. Sun, "Deep residual learning for image recognition," in *Proc. Comput. Vision and Pattern Recognition*, 2016, pp. 770–778. [Online]. Available: <http://arxiv.org/abs/1512.03385>
- [5] F. N. Iandola, S. Han, M. W. Moskewicz, K. Ashraf, W. J. Dally, and K. Keutzer. (2016) SqueezeNet: AlexNet-level accuracy with 50x fewer parameters and <0.5MB model size. [Online]. Available: <http://arxiv.org/abs/1602.07360>
- [6] P. Sermanet, D. Eigen, X. Zhang, M. Mathieu, R. Fergus, and Y. LeCun, "OverFeat: Integrated recognition, localization and detection using convolutional networks," in *Proc. Int. Conf. Learning Representations*, 2014. [Online]. Available: <http://arxiv.org/abs/1312.6229>
- [7] R. Girshick, J. Donahue, T. Darrell, and J. Malik, "Rich feature hierarchies for accurate object detection and semantic segmentation," in *Proc. Comput. Vision and Pattern Recognition*, 2014, pp. 580–587.
- [8] R. Girshick, "Fast R-CNN," in *Proc. Int. Conf. Comput. Vision*, 2015, pp. 1440–1448. [Online]. Available: <http://arxiv.org/abs/1504.08083>
- [9] S. Ren, K. He, R. Girshick, and J. Sun, "Faster R-CNN: Towards real-time object detection with region proposal networks," in *Proc. Advances in Neural Inf. Process. Syst.*, 2015, pp. 1–9.
- [10] N. McLaughlin, J. M. del Rincon, and P. C. Miller, "Person reidentification using deep convnets with multitask learning," *IEEE Trans. Circuits Syst. Video Technol.*, vol. 27, no. 3, pp. 525–539, Mar. 2017.
- [11] J. Long, E. Shelhamer, and T. Darrell, "Fully convolutional networks for semantic segmentation," in *Proc. Comput. Vision and Pattern Recognition*, 2015. [Online]. Available: <http://arxiv.org/abs/1411.4038>
- [12] T. Chen, Z. Du, N. Sun, J. Wang, C. Wu, Y. Chen, and O. Temam, "DianNao: A small-footprint high-throughput accelerator for ubiquitous machine-learning," in *Proc. Int. Conf. Architectural Support for Programming Languages and Operating Syst.*, 2014, pp. 269–283.
- [13] J. Albericio, P. Judd, T. Hetherington, T. Aamodt, N. E. Jerger, and A. Moshovos, "Cnvlutin: Ineffectual-neuron-free deep neural network computing," in *Proc. Int. Symp. Comput. Architecture*, 2016, pp. 1–13.

- [14] C. Zhang, P. Li, G. Sun, Y. Guan, B. Xiao, and J. Cong, "Optimizing FPGA-based accelerator design for deep convolutional neural networks," in *Proc. ACM/SIGDA Int. Symp. Field Programmable Gate Arrays*, 2015, pp. 161–170.
- [15] L. Song, Y. Wang, Y. Han, X. Zhao, B. Liu, and X. Li, "C-Brain: A deep learning accelerator that tames the diversity of CNNs through adaptive data-level parallelization," in *Proc. Design Automation Conf.*, 2016, pp. 123:1–123:6.
- [16] J. Qiu, J. Wang, S. Yao, K. Guo, B. Li, E. Zhou, J. Yu, T. Tang, N. Xu, S. Song, Y. Wang, and H. Yang, "Going deeper with embedded FPGA platform for convolutional neural network," in *Proc. ACM/SIGDA Int. Symp. Field Programmable Gate Arrays*, 2016, pp. 26–35.
- [17] M. Motamedi, P. Gysel, V. Akella, and S. Ghiasi, "Design space exploration of FPGA-based deep convolutional neural networks," in *Proc. Asia and South Pacific Design Automation Conf.*, 2016, pp. 575–580.
- [18] J. Jo, S. Cha, D. Rho, and I.-C. Park, "DSIP: A scalable inference accelerator for convolutional neural networks," *IEEE J. Solid-State Circuits*, vol. 53, no. 2, pp. 605–618, Feb. 2018.
- [19] S. Han, J. Pool, J. Tran, and W. J. Dally, "Learning both weights and connections for efficient neural networks," in *Proc. Advances in Neural Inf. Process. Syst.*, 2015, pp. 1135–1143. [Online]. Available: <http://arxiv.org/abs/1506.02626>
- [20] S. Han, H. Mao, and W. J. Dally, "Deep Compression: Compressing deep neural networks with pruning, trained quantization and Huffman coding," in *Proc. Int. Conf. Learning Representations*, 2016. [Online]. Available: <http://arxiv.org/abs/1510.00149>
- [21] T.-J. Yang, Y.-H. Chen, and V. Sze, "Designing energy-efficient convolutional neural networks using energy-aware pruning," in *Proc. Comput. Vision and Pattern Recognition*, 2017. [Online]. Available: <http://arxiv.org/abs/1611.05128>
- [22] W. Wen, C. Wu, Y. Wang, Y. Chen, and H. Li, "Learning structured sparsity in deep neural networks," in *Proc. Advances in Neural Inf. Process. Syst.*, 2016, pp. 2074–2082.
- [23] H. Li, A. Kadav, I. Durdanovic, H. Samet, and H. P. Graf, "Pruning filters for efficient ConvNets," in *Proc. Int. Conf. Learning Representations*, 2017. [Online]. Available: <http://arxiv.org/abs/1608.08710>
- [24] Y. He, X. Zhang, and J. Sun, "Channel pruning for accelerating very deep neural networks," in *Proc. Int. Conf. Comput. Vision*, 2017, pp. 1398–1406. [Online]. Available: <http://arxiv.org/abs/1707.06168>
- [25] J. Yu, A. Lukefahr, D. Palframan, G. Dasika, R. Das, and S. Mahlke, "Scalpel: Customizing DNN pruning to the underlying hardware parallelism," in *Proc. Int. Symp. Comput. Architecture*, 2017, pp. 548–560.
- [26] P. Molchanov, S. Tyree, T. Karras, T. Aila, and J. Kautz, "Pruning convolutional neural networks for resource efficient inference," in *Proc. Int. Conf. Learning Representations*, 2017. [Online]. Available: <http://arxiv.org/abs/1611.06440>
- [27] N. Yu, S. Qiu, X. Hu, and J. Li, "Accelerating convolutional neural networks by group-wise 2D-filter pruning," in *Proc. Int. Joint Conf. Neural Networks*, 2017, pp. 2502–2509.
- [28] V. Lebedev and V. Lempitsky, "Fast ConvNets using group-wise brain damage," in *Proc. Comput. Vision and Pattern Recognition*, 2016, pp. 2554–2564. [Online]. Available: <http://arxiv.org/abs/1506.02515>
- [29] S. Anwar, K. Hwang, and W. Sung, "Structured pruning of deep convolutional neural networks," *ACM J. on Emerging Technologies in Computing Syst.*, vol. 13, no. 3, pp. 32:1–32:18, feb 2017.
- [30] H. Mao, S. Han, J. Pool, W. Li, X. Liu, Y. Wang, and W. J. Dally, "Exploring the regularity of sparse structure in convolutional neural networks," in *Proc. Int. Conf. Learning Representations*, 2017. [Online]. Available: <http://arxiv.org/abs/1705.08922>
- [31] D. Kadetotad, S. Arunachalam, C. Chakrabarti, and J.-S. Seo, "Efficient memory compression in deep neural networks using coarse-grain sparsification for speech applications," in *Proc. Int. Conf. Comput. Aided Design*, 2016.
- [32] J. Park, S. Li, W. Wen, P. T. P. Tang, H. Li, Y. Chen, and P. Dubey, "Faster CNNs with direct sparse convolutions and guided pruning," in *Proc. Int. Conf. Learning Representations*, 2017.
- [33] Y. Boo and W. Sung, "Structured sparse ternary weight coding of deep neural networks for efficient hardware implementations," in *Proc. IEEE Workshop on Signal Process. Syst. Design and Implementation*, 2017.
- [34] S. Han, X. Liu, H. Mao, J. Pu, A. Pedram, M. A. Horowitz, and W. J. Dally, "EIE: Efficient inference engine on compressed deep neural network," in *Proc. Int. Symp. Comput. Architecture*, 2016, pp. 243–254. [Online]. Available: <http://arxiv.org/abs/1602.01528>
- [35] S. Han, J. Kang, H. Mao, Y. Hu, X. Li, Y. Li, D. Xie, H. Luo, S. Yao, Y. Wang, H. Yang, and W. J. Dally, "ESE: Efficient speech recognition engine with sparse LSTM on FPGA," in *Proc. ACM/SIGDA Int. Symp. Field Programmable Gate Arrays*, 2017, pp. 75–84.
- [36] S. Zhang, Z. Du, L. Zhang, H. Lan, S. Liu, L. Li, Q. Guo, T. Chen, and Y. Chyen, "Cambricon-X: An accelerator for sparse neural networks," in *Proc. Int. Symp. Micro-architecture*, 2016, pp. 20:1–20:12.
- [37] A. Parashar, M. Rhu, A. Mukkara, A. Puglielli, R. Venkatesan, B. Khailany, J. Emer, S. W. Keckler, and W. J. Dally, "SCNN: An accelerator for compressed-sparse convolutional neural networks," in *Proc. Int. Symp. Comput. Architecture*, 2017.
- [38] D. Kim, J. Ahn, and S. Yoo, "A novel zero weight/activation-aware hardware architecture of convolutional neural network," in *Proc. Design, Automation & Test in Europe Conf. & Exhibition*, 2017, pp. 1462–1467.
- [39] Y. LeCun, J. S. Denker, and S. A. Solla, "Optimal brain damage," in *Proc. Advances in Neural Inf. Process. Syst.*, 1990, pp. 598–605.
- [40] B. Hassibi and D. G. Stork, "Second order derivatives for network pruning: Optimal brain surgeon," in *Proc. Advances in Neural Inf. Process. Syst.*, 1993, pp. 164–171.
- [41] B. Hassibi, D. G. Stork, and G. J. Wolff, "Optimal brain surgeon and general network pruning," in *Proc. Int. Conf. Neural Networks*, 1993, pp. 293–299.
- [42] O. Russakovsky, J. Deng, H. Su, J. Krause, S. Satheesh, Z. Ma, S. a. dn Huang, A. Karpathy, A. Khosla, M. Bernstein, A. C. Berg, and L. Fei-Fei, "ImageNet large scale visual recognition challenge," *Int. J. Comput. Vision*, vol. 115, no. 3, pp. 211–252, Dec. 2015.
- [43] Y. Jia, E. Shelhamer, J. Donahue, S. Karayev, J. Long, R. Girshick, S. Guadarrama, and T. Darrel. (2014) Caffe: Convolutional architecture for fast feature embedding. [Online]. Available: <http://arxiv.org/abs/1408.5093>
- [44] Y. Jia, E. Shelhamer, J. Donahue, S. Karayev, J. Long, R. Girshick, S. Guadarrama, and T. Darrell. Caffe. [Online]. Available: <https://github.com/BVLC/caffe>
- [45] K. Simonyan and A. Zisserman. VGG16/19. [Online]. Available: http://www.robots.ox.ac.uk/~fvg/research/very_deep
- [46] K. He, X. Zhang, S. Ren, and J. Sun. ResNet. [Online]. Available: <https://github.com/KaimingHe/deep-residual-networks>
- [47] F. N. Iandola, S. Han, M. W. Moskewicz, K. Ashraf, W. J. Dally, and K. Keutzer. SqueezeNet. [Online]. Available: <https://github.com/DropScale/SqueezeNet>
- [48] MobileNet caffe model. [Online]. Available: <https://github.com/shicai/MobileNet-Caffe>
- [49] A. G. Howard, M. Zhu, B. Chen, D. Kalenichenki, W. Wang, T. Weyand, M. Andreetto, and H. Adam. (2017) MobileNets: Efficient convolutional neural networks for mobile vision applications. [Online]. Available: <http://arxiv.org/abs/1704.04861>
- [50] X. Zhang, X. Zhou, M. Lin, and J. Sun, "ShuffleNet: An extremely efficient convolutional neural network for mobile devices," in *Proc. Comput. Vision and Pattern Recognition*, 2018. [Online]. Available: <http://arxiv.org/abs/1707.01083>
- [51] Y. He, X. Zhang, and J. Sun. Channel pruning for accelerating very deep neural networks. [Online]. Available: <https://github.com/yihui-he/channel-pruning>